Developmental Biology **224,** 138–151 (2000)
doi:10.1006/dbio.2000.9779, available online at http://www.idealibrary.com on IDEAL®

Embryonic Origins of Auditory Brain-Stem Nuclei in the Chick Hindbrain

Karina S. Cramer,* Scott E. Fraser,† and Edwin W Rubel*

**Virginia Merrill Bloedel Hearing Research Center, Department of Otolaryngology and Head and Neck Surgery, University of Washington, Seattle, Washington 98195; and †Beckman Institute, California Institute of Technology, Pasadena, California 91125*

The auditory nuclei of the chick brain stem have distinct morphologies and highly specific synaptic connectivity. Nucleus magnocellularis (NM) and nucleus angularis receive tonotopically ordered cochlear input. NM in turn projects tonotopically to nucleus laminaris (NL), maintaining binaural specificity with projections to either dorsal or ventral NL dendrites. NM and NL arise from a common anlage, which differentiates as the cells migrate and acquire their mature morphologies. NM and NL cells are closely associated during embryogenesis and synapse formation. However, the morphologies of the nuclei and of the cells within the nuclei differ greatly between NM and NL. While later maturation of these nuclei has been described in considerable detail, relatively little is known about the early embryonic events that lead to the formation of these nuclei. We examined the embryonic origins of cells in brain-stem auditory nuclei with particular emphasis on NM and NL. Lipophilic dyes were injected into small regions of the embryonic hindbrain prior to the birth and migration of cells that contribute to these nuclei. We found that NM arises from rhombomeres r5, r6, and r7, and NL arises mostly from r5 with a few cells arising from r6. NM and NL thus have partially overlapping rhombomeres of origin. However, we found that the precursors for NM and NL are found in distinct regions within rhombomere 5, with NM precursors in medial regions and NL precursors in lateral regions. Our results do not support a lineage relationship between NM and NL cells and they suggest that NM and NL are specified prior to migration of precursors to the auditory anlage.

Key Words: **hindbrain; auditory brain stem; nucleus laminaris; nucleus magnocellularis; fate map.**

INTRODUCTION

The auditory brain-stem nuclei in the chick have distinct morphologies and display a highly precise pattern of synaptic connections whose function in auditory processing has been characterized (Rubel and Parks, 1988). Calyceal inputs from the basilar papilla (cochlea) originating from the VIIIth nerve (Parks and Rubel, 1978; Parks, 1981) project topographically onto neurons of ipsilateral nucleus magnocellularis (NM), preserving the orderly array of frequency tuning found in the sensory epithelium. Collateral branches of VIIIth nerve axons also make synapses onto neurons of nucleus angularis (NA). NM neurons are large and have few dendritic processes in mature birds. NM projects bilaterally and tonotopically to nucleus laminaris (NL), a thin lamina of cells with bitufted dendritic morphology (Parks and Rubel, 1975; Rubel and Parks, 1975; Smith and Rubel, 1979; Jhaveri and Morest, 1982b; Young and Rubel, 1983). Ipsilateral NM projections terminate on cell bodies and dorsal NL dendrites, while contralateral NM projections terminate on cell bodies and ventral NL dendrites (Parks and Rubel, 1975; Hackett *et al.*, 1982; Jhaveri and Morest, 1982b; Young and Rubel, 1983). This pattern of connectivity establishes an orderly representation of interaural time differences for all frequencies. These computations may enable the animal to localize sounds in space (Young and Rubel, 1983; Takahashi *et al.*, 1984; Sullivan and Konishi, 1986; Overholt *et al.*, 1992; Schwarz, 1992). Neurons in NL and NA project topographically to the superior olivary nucleus (SON) (Moiseff and Konishi, 1983; Lachica *et al.*, 1994), which in turn makes inhibitory connections with neurons in ipsilateral NA, NM, and NL (Takahashi and Konishi, 1988; Carr *et al.*, 1989; Carr and Boudreau, 1993; Westerberg and Schwarz, 1995; Yang *et al.*, 1999; Monsivais *et al.*, 2000). The developmental mechanisms that specify these nuclei and their synaptic connections are not known. However, this system affords an opportunity to study neural development in relation to mature function. While many of the later developmental events in this system have been described (Rubel *et al.*, 1976; Rubel, 1978; Rubel and Parks, 1988), relatively little is known about the early embryonic events that lead to the formation of these nuclei and the maturation of cells that make up the nuclei.

0012-1606/00 $35.00

TABLE 1
Dye Injections into Whole Rhombomeres

Rhombomere injected	Age at injection	Size of injection	Nuclei labeled
r4	E2.5	150	NA, VeL, SON, VeM
r4	E2.5	200	NA, VeL, VeM
r4	E2.5	120	NA, VeL
r4	E2	100	NA, VeL
r5	E2.5	200	NM, NL, NA, SON, VeL, VeM, VeD
r5	E2.5	50	NM, NL
r6	E2.5	100	NM, NL, NA, VeM, VeD
r6	E2.5	80	NM, few NL cells
r6	E2	50	NM, NL
r6	E2	75	few NM cells
r7	E2	70	caudal NM, VeM
r7	E2	75	caudal NM
r7	E2.5	80	no NM or NL

Note. Labeled nuclei were identified in sections from E9–E12 brain stems. Abbreviations: NA, n. angularis; NL, n. laminaris; NM, n. magnocellularis; SON, superior olivary nucleus; VeL, lateral vestibular nucleus; VeM, medial vestibular nucleus; VeD, dorsal vestibular nucleus.

The vertebrate brain stem derives from the hindbrain, which is morphologically segmented into neuromeres known as rhombomeres (Vaage, 1969). In the chick, rhombomere boundaries are first seen at about 2 days of incubation (E2) and are no longer evident after about E5 (Vaage, 1969). These segments display a precise pattern of gene expression (Wilkinson *et al.*, 1989; Hunt and Krumlauf, 1992; McKay *et al.*, 1994; Nonchev *et al.*, 1996). Boundaries between rhombomeres are specialized and limit migration of cells between rhombomeres (Fraser *et al.*, 1990). Birthdating studies using tritiated thymidine have shown that neurons in NM are born at E2.5 to E3, while NL cells are born between E3.5 and E4 (Rubel *et al.*, 1976). The first sign of the developing auditory nuclei is the formation of the auditory anlage, a transient structure that is present at E6–7 and located in a lateral and dorsal position within the developing brain stem (Harkmark, 1954; Book and Morest, 1990). NM and NL become distinct from each other as NL cells move ventrally, beginning at E7, and both nuclei migrate medially to their final positions near the midline by about E12. NM and NL thus acquire their distinctive morphologies and synaptic connectivity from an anlage in which cell fate is as yet indistinguishable. What are the mechanisms that specify this differentiation? Because the two nuclei form a common anlage, it is possible that some progenitor cells give rise to cells in both NM and NL (Rubel *et al.*, 1976). However, the neurons in these nuclei are quite distinct, and thus an interesting possibility is that they arise from two distinct pools of precursors (Marin and Puelles, 1995). In this study, we have investigated the fate map of the early hindbrain in order to address this question.

Two previous studies have examined the fates of cells in rhombomeres in relation to brain-stem nuclei. These studies used quail/chick chimeras to identify regions of the hindbrain that contribute to mature nuclei within the brain stem. Transplants of alar and basal regions of neural tube (Tan and Le Douarin, 1991) showed that sensory nuclei arise from alar (dorsal) neural tube; these nuclei include NM and NL. A study of grafts involving single rhombomeres (Marin and Puelles, 1995) identified the rhombomeric origins of nuclei in the avian brain stem. Their study showed that NM and NL both arise from more than one rhombomere, and that they both arise from precursors within rhombomere 6. In the present study we have examined this issue in detail. We used small injections of lipophilic dyes (Fraser, 1996) to reliably label cells within rhombomeres early in development, just prior to the final mitotic divisions that give rise to NM. We then examined the distribution of labeled cells in the brain stem after the auditory brain-stem nuclei had formed. This method allowed us to use a minimally invasive technique to examine the fate map of the hindbrain. More importantly, it allowed us to examine the embryonic origins of the auditory brainstem nuclei at the level of small regions within rhombomeres and to double label small groups of cells within rhombomeres. Our results show that NM and NL neurons arise from overlapping sets of rhombomeres. However, precursors for NM and NL are in distinct locations within rhombomeres. Moreover, we found a systematic relationship between the positions of precursors within rhom-

FIG. 1. DiI injection into r4. (A) An E2 embryo, immediately following injection of DiI into left r4. The arrow indicates injection site. Arrowheads indicate rhombomere boundaries. Scale bar, 500 μm. (B) Fluorescence image of an E10 rostral brain-stem section in the same embryo that is shown in A. This coronal section is rostral to NM and NL. Labeling appears as a medial streak that expands laterally in ventral regions. Only the left (injected) side is labeled. Scale bar, 200 μm, also applies to C. (C) DiI labeling in a rostral section from the same brain stem containing NM and NL. NM and NL are not labeled by this r4 injection. Labeled areas are positioned more laterally than in more rostral sections. (D) Higher magnification of labeling in a middle section. NA is labeled. Scale bar, 100 μm.

FIG. 2. DiI injection into r5. (A) An E2.5 embryo, immediately following injection of r5 with DiI. The arrow indicates the injection site. As this embryo has begun to turn, the otocyst is visible just below the injection site, and the r5/r6 boundary is midway through the otocyst. (B) At E10, DiI labeling in this embryo is abundant in this section rostral to NM and NL. Scale bar, 100 μm. (C) Section through the brain-stem region containing the rostral part of NM and NL. Cells in both NM and NL are abundantly labeled. Scale bar, 50 μm. (D) Caudal section through this brain stem. NM cells are labeled along with a large region in the lateral brain stem. Scale bar, 100 μm.

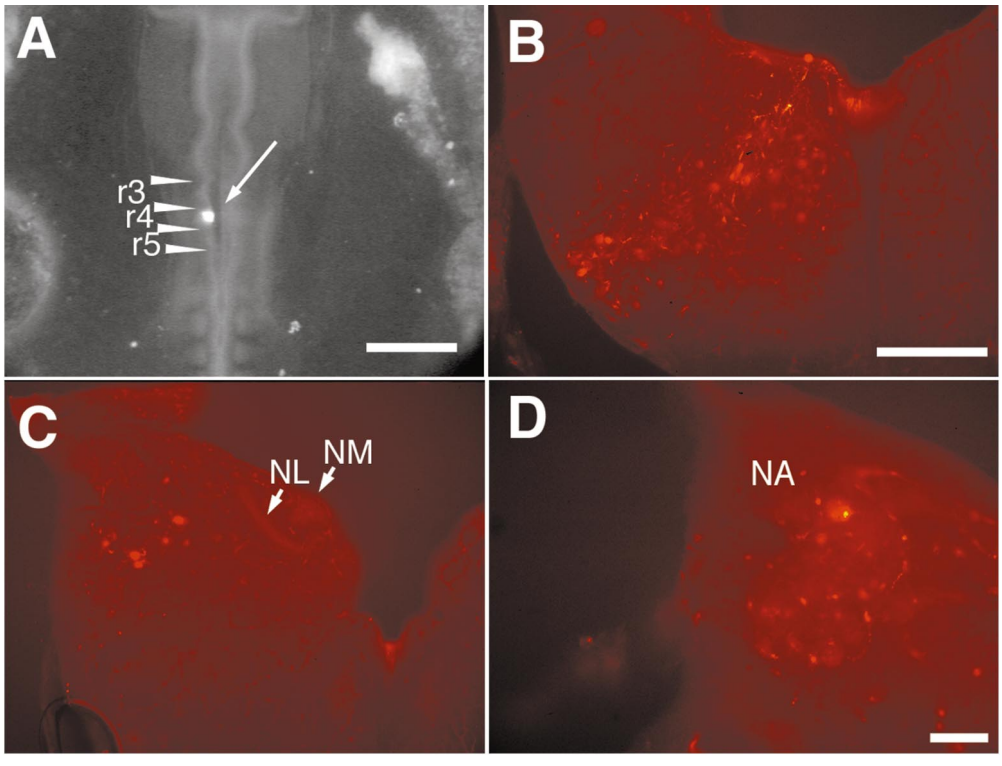

1

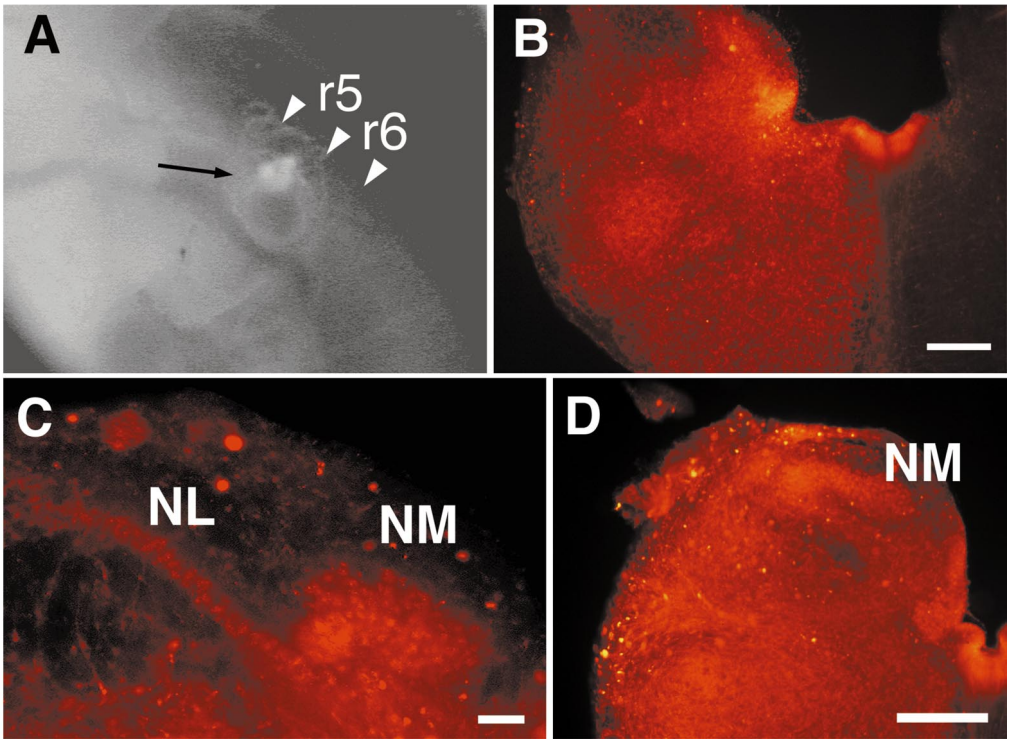

2

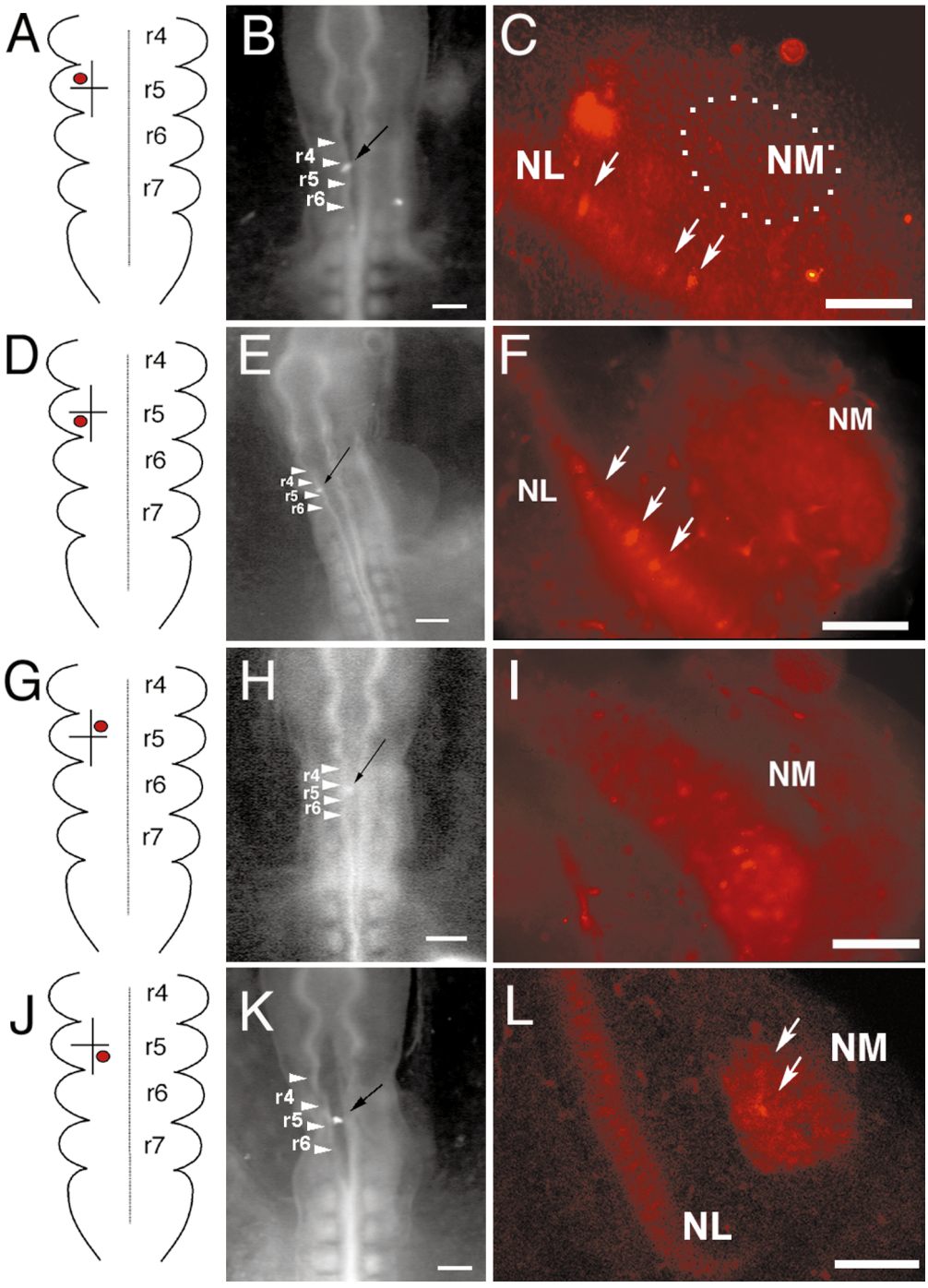

FIG. 3. Injections of DiI into r5 quadrants. (A) Schematic illustration of E2 hindbrain, with injection position noted. Quadrants were either medial or lateral and either anterior or posterior. A lateral anterior position on the left side of the hindbrain is shown. (B) Fluorescent digital image of an E2 embryo following pressure injection of DiI into the lateral anterior quadrant of left r5 (black arrow). Arrowheads indicate rhombomere boundaries. (C) Coronal brain-stem section from the same embryo at E12 reveals DiI labeling in NL (white arrows) but not in NM in the left half of the section. Dotted lines show boundaries of NM based on bisbenzimide counterstaining. (D) Schematic illustration of an injection into the lateral posterior quadrant of left r5. (E) An embryo injected with DiI in the lateral posterior quadrant of left r5 at E2. (F) Brain-stem section from the embryo shown in E after survival to E12. Labeled cells are found in NL (white arrows) but not in NM on the left side of the brain stem. (G) Schematic illustration of injection into the medial anterior quadrant of left r5. (H) An E2 embryo injected with DiI into the medial anterior quadrant of left r5. (I) The left side of a caudal section through the brain stem of the embryo shown in H, after survival to E12. DiI-labeled cells are found in NM but not in NL. (J) A schematic illustration of an injection in the medial posterior quadrant of r5. (K) An E2 embryo after injection of DiI into the medial posterior quadrant of left r5. (L) Same embryo as in K, confocal image of left side of a brain-stem section at E12. Labeled cells are found in NM (white arrows), but not in NL. Scale bars in B, E, H, and K, 200 μm. Scale bars in C, F, I, and L, 100 μm.

bomeres and the positions of cells within nuclei NM and NL. This relationship was preserved along both the rostrocaudal and the mediolateral axes. These findings suggest that precursors for NM and NL are specified early in development. Because the precursors are at distinct locations prior to their birth dates and are in distinct nuclei after migration is complete, it is possible that they follow distinct migratory pathways during the maturation of the auditory brain stem.

MATERIALS AND METHODS

Rhombomere Injections

Fertilized White Leghorn chicken eggs (*Gallus domesticus*) were obtained from H&N International (Redmond, WA) and were incubated in a forced-air incubator at 38°C. Embryos were injected at E2. At E2, eggs were removed and swabbed with 70% ethanol. Eggs were equilibrated on their sides and plastic tape was placed over the top. Eggs were windowed using a modification of published methods (Fraser, 1996). A small hole was made in the large end of the shell, and 2.5–5 ml of albumin was removed with a 5-ml syringe and a sterile 18-gauge needle. Another small hole was made in the taped region to allow the embryo to sink below the shell. A window (about 2 cm in diameter) was cut through the taped region using small scissors, leaving a small portion intact so that the window was a flap that could be resealed. The egg was placed on a small wax ring on the stage of a dissecting microscope. A 26-gauge needle was used to inject a small amount of India ink (30% in sterile phosphate-buffered saline (PBS), containing 10 mM Na/K phosphate buffer and 150 mM NaCl, pH 7.4) below the embryo to provide contrast for adequate visualization of the embryonic hindbrain and to allow for accurate staging of the embryo.

Embryos were typically at Hamburger–Hamilton stage (HH) 12–15 at the time of injection (Hamburger and Hamilton, 1951). At these stages, rhombomere boundaries can be clearly identified (Vaage, 1969). In particular, the rhombomere 5/6 boundary was adjacent to the approximate center of the otocyst. Additionally, the characteristic morphology and opaque hue of rhombomere 4 were also used to identify rhombomeres and rhombomere boundaries. The vitelline membrane overlying the embryo was removed using fine tungsten needles. In some cases, the amniotic sac covered the hindbrain region and was gently opened as well. In addition, in some cases the IVth ventricle was opened in a small area over the rhombomere to be injected, so that the boundaries were visible and so that areas within rhombomeres could be injected accurately.

Micropipettes were pulled on a Brown Flaming puller and broken so that the tip diameter was approximately 10 μm. They were then filled with dye using a pulled 1-ml syringe. Most injections were made using 5% DiI CM Cell Tracker (Molecular Probes, Eugene, OR), a lipophilic carbocyanine dye that appears red under epifluorescence illumination. DiI was prepared in 100% ethanol and then diluted in 10% sterile sucrose. This vehicle seemed to give a solution that did not precipitate easily upon contact with the tissue. Some injections were made using other lipophilic dyes. These were 5% DiO (green) in 100% ethanol or 5% DiD (far red) in 100% ethanol. Pressure injections were made using a Picospritzer II (General Valve Corp., East Hanover, NJ) through the micropipette filled with dye solution. We used a hydraulic micromanipulator to position the micropipette over the region to be injected. The micropipette was lowered into the rhombomere and a pressure of 5–10 p.s.i. was applied for 20–50 ms. The location of the injection was verified and documented using a Leitz MZFLIII dissecting microscope equipped with epifluorescence to view the fluorescent dyes. A single-chip CCD digital camera mounted on the microscope was used to capture an image of the injection site within the embryo using Scion Image software (NIH) and a Macintosh computer. After the image was recorded, the window on the egg was taped closed. The egg was then placed into a humid 38°C tabletop incubator for 5 to 11 days.

Histology

Eggs were removed from the incubator, and embryos were dissected and staged using Hamburger–Hamilton criteria. Brain stems were dissected free in PBS and then transferred to a solution of 4% paraformaldehyde in PBS. Tissue was fixed overnight and then rinsed several times in PBS. Brain stems were embedded in 2–4% agarose and cut at 100 μm in the coronal plane on a Vibratome tissue slicer (Pelco, St. Louis, MO). All serial sections were saved. In some cases sections were counterstained with a 5- to 10-min incubation in bisbenzimide followed by several rinses in PBS. Sections were placed in DABCO in glycerol/PBS, then mounted in DABCO (to prevent bleaching of fluorescence) in glycerol, and coverslipped. Tissue was examined on a Leica epifluorescence microscope with appropriate filter sets for DiI, DiO, or bisbenzimide. Because the tissue was cleared in glycerol, nuclear boundaries and the locations of labeled cells in these relatively thick sections could be discerned with standard epifluorescence microscopy. Auditory brain-stem nuclei were often identifiable with DiI viewing alone because background fluorescence highlighted the boundaries of NM and NL. Nomarski optics and/or bisbenzimide staining aided in this identification. In addition, a BioRad 1024 confocal microscope was used in several cases in order to optically section through the tissue.

Sections throughout the rostrocaudal extent of the brain-stem auditory nuclei were examined, and the locations of all labeled cells in the auditory nuclei were noted. The following criteria were used to define the rostrocaudal locations of labeled cells: *Rostral* sections contained the anterior portion of NL and NM and also contained regions of NA and SON. After approximately E10 (HH stage 36), NL appears in rostral sections as a line of cells running primarily dorsoventrally, and NM is medial to NL. NA is at the lateral edge of these sections. NM, NL, and NA all lie near the dorsal surface. SON is in the ventral region of these sections, lateral to NL and medial to NA. *Middle* sections were also through a region of the brain stem containing both NM and NL, but in these sections NL courses mediolaterally, and NM is located dorsal to NL. SON is present in middle sections in a position similar to that seen in rostral sections. *Caudal* sections contained NM but not NL. Representative sections from labeled brain stems were photographed with conventional or digital photomicrography shortly after sectioning.

Analysis of Rostrocaudal Topography

We assessed the relationship between the rostrocaudal position of the injection at E2–E2.5 and the rostrocaudal position of labeled NM and NL cells within the sections through the auditory brainstem nuclei at E9–12. For this analysis, the injection sites at E2 were assigned positional values as follows: r5 rostral, 1; r5 rostral and caudal, 1.5; r5 caudal, 2; r6 rostral, 3; r6 rostral and caudal, 3.5; r6 caudal, 4; and r7, 5. In E9–E12 material, sections from all levels containing NM or NL were assessed for DiI label. The presence of

labeled cells in NM or NL was rated as 0 (no label), 1 (small amount of label), or 2 (significant label); these scores (S) were assigned for each rostrocaudal level. A rostrocaudal labeling index was then computed separately for NM and NL. Sections containing NL were either rostral (r, position value 1) or middle (m, position value 2). Sections containing NM were rostral, middle, or caudal (assigned positional values of 1 to 3). The index (I) reflected the average position of labeled cells within the brain stem at E9–E12:

$$I_{NL} = [S_{NL,r}(1) + S_{NL,m}(2)]/[S_{NL,r} + S_{NL,m}]$$

$$I_{NM} = [S_{NM,r}(1) + S_{NM,m}(2) + S_{NM,c}(3)]/[S_{NM,r} + S_{NM,m} + S_{NM,c}].$$

I_{NL} ranges from 1 to 2, and I_{NM} ranges from 1 to 3, with small values more caudal and greater values more rostral. The index is defined only when labeling is present in the nucleus. A comparison between injection position and position of label in the auditory brain-stem nuclei was performed using Spearman's correlation assuming the variables are continuous. As the rostrocaudal labeling indices were computed separately for NL and NM, the analysis was computed separately for NL labeling and NM labeling. We began to make these measurements after the fate mapping study had begun; thus these analyses were performed on a subset of our brain-stem tissue. A total of 28 embryos were analyzed for rostrocaudal topography.

RESULTS

A total of 44 embryos with 48 dye injections were included in the analysis. Inclusion criteria were: (1) clearly identifiable injection site that did not extend across rhombomere boundaries; (2) survival to E9–12, at which time NM and NL have differentiated and can be readily identified; and (3) evidence of dye labeling in at least some regions of the brain stem in coronal sections.

Injection sizes were measured in 43 cases (43 injections from 40 embryos) using a digitized image of the labeled embryo calibrated with a stage micrometer. Some injections were intended to label the entire area within one side of a rhombomere; for simplicity we will use the term rhombomere to indicate hemirhombomere. The rostrocaudal extent of a rhombomere was about 120 μm at E2 and grew to 200 μm at E2.5. Accordingly, rhombomere injections had a mean diameter of 104 ± 51 μm (SD, n = 13) and thus on average covered the majority of the surface of the rhombomere. A summary of rhombomere injection sizes and results from fate mapping is presented in Table 1. The two largest injections, 200 μm each, were both made in E2.5 embryos in which rhombomeres are at the largest end of the range used in this study. Because both the injection site and the rhombomere boundaries were visible at the time of injection, we were able to discard any cases in which the dye extended across a rhombomere boundary.

Other injections were intended to be restricted to an area within a half or a quadrant of a rhombomere. The diameters of injections confined to a quadrant of a rhombomere averaged 37 ± 14 μm (n = 23). These injections were restricted within either the rostral or the caudal portion of the rhombomere and within either the lateral or the medial portion of the rhombomere. The average diameter of injections confined to half of a rhombomere was 44 ± 16 μm (n = 7); these were confined to either the lateral or the medial portion of the rhombomere. In some cases the embryos were examined under the fluorescence dissecting microscope again 24 h after injection to verify that the dye remained visible and restricted within the original site. The spread of dye at this time was very limited and remained within the region originally injected.

Labeling with DiI at E9–E12 resulted in bright punctate labeling within cell bodies. Often fibers and blood vessels were also discernible. The region of label for most injections was medial in rostral sections and progressively more lateral in more caudal sections. In younger embryos (E7) labeling in what appeared to be axons was also evident, but in E9–12 embryos axonal labeling was difficult to discern. The distribution of label at E9–12 following injections into confined regions within the hindbrain is described below.

Rhombomere 4

Injections of DiI into r4 (n = 4) were fairly large and were intended to label most of the rhombomere. Brain-stem sections were examined at E9–E12, when NM and NL can be identified in coronal sections. An example of an injection in r4 and the resulting label is shown in Fig. 1. Labeled cells were evident in sections rostral to NM and NL (Fig. 1B). The large strips of label spanned the dorsoventral extent of the sections, particularly in rostral sections. In general, regions of label were progressively more lateral in more caudal sections. R4 injections did not result in labeled cells in the auditory brain-stem nuclei NM and NL (Fig. 1C). However, labeled cells were evident in NA (Fig. 1D), in the lateral vestibular nucleus (VeL), the medial vestibular nucleus (VeM), the tangential nucleus, the nucleus of the VIIth nerve, and in one case, in SON (Table 1).

Rhombomere 5

Large injections into rhombomere r5 (n = 2) resulted in labeling in both NM and NL. An example is shown in Fig. 2. Figure 2A shows the embryo after an injection was made into r5. Rostral (Fig. 2B), middle (Fig. 2C), and caudal (Fig. 2D) sections through this brain stem show DiI labeling in numerous other nuclei in addition to NM and NL. Within the auditory system, r5 injections resulted in labeled NA and SON neurons as well. In addition (see Table 1), labeling was present in VeM, VeL, the dorsal vestibular nucleus (VeD), and the tangential nucleus.

In many cases, small injections of DiI did not label both NM and NL, suggesting a finer organization to the fates of the cells within r5. To assess this possibility, we made small DiI injections that were contained within one of four quadrants of r5. The labeled descendants were found to be largely distinct. Representative examples of our findings from these small injections are shown in Figs. 3 and 4.

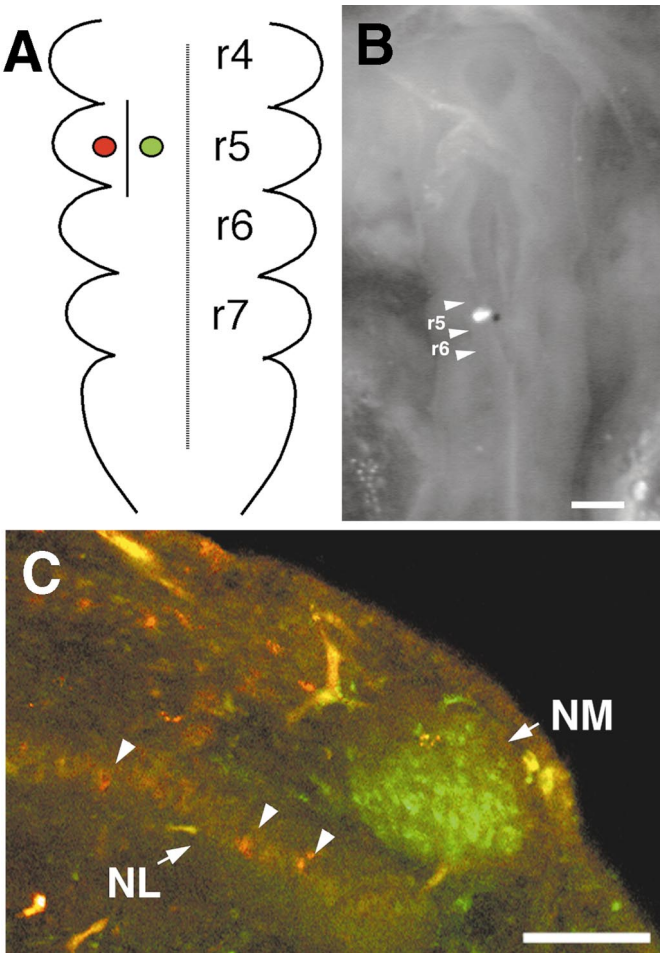

FIG. 4. Precursors for NM and NL are located in distinct regions of r5. (A) Schematic illustration of placement of two different dyes into r5. The red dye is placed in the lateral half of the rhombomere and the green dye is placed in the medial half. (B) An E2 embryo after injection of DiI (bright spot) in the lateral half of left r5 and of DiD (dark spot) in the medial half of the same rhombomere. Scale bar, 200 μm. (C) Confocal microscopy image of the left side of a brain-stem section of the embryo shown in B after survival to E9. Arrowheads indicate DiI (red)-labeled cells in NL. Green areas represent DiD labeling, seen abundantly in NM. Scale bar, 100 μm.

Figure 3A shows a schematic diagram illustrating the position of a small DiI injection into the lateral anterior quadrant of r5 (n = 5). A digital photomicrograph taken at the time of injection (E2) is shown in Fig. 3B. The resulting DiI labeling at E12 (Fig. 3C) is found in NL and in other regions of the brain stem but not in NM. Similarly, lateral posterior r5 injections (n = 4; Figs. 3D and 3E) resulted in label in NL but not in NM (Fig. 3F). In contrast, medial anterior injections in r5 (n = 3; Figs. 3G and 3H) consistently labeled cells in NM but resulted in little or no label in NL. Figure 3I shows labeling of NM in a caudal section through the brain stem of the embryo shown in Fig. 3H. Many NM cells are labeled with DiI. NL, not shown in this caudal section, is not labeled. R5 injections into the medial posterior quadrant of r5 (n = 4; Figs. 3J and 3K) also resulted in label in NM cells but not in NL cells (Fig. 3L). Table 2 summarizes the results of injections into alar plate regions of r5 with respect to contributions to NM and NL. No lateral r5 injections (n = 13) resulted in labeled NM neurons, and 11 resulted in labeled NL neurons. All medial injections (n = 10) resulted in label in NM, while only 2 resulted in any labeled cells in NL. All of these injections were made into the lateral and medial portions of the alar plate. In a few cases, medial injections were made toward the midline and were most likely in the basal plate. These injections did not result in label in either NM or NL (data not shown), consistent with the results of Tan and LeDouarin (1991). Thus, results from r5 injections suggest that the precursors for NM and NL are abundantly present in r5 but at E2 are spatially segregated within the rhombomere.

To further assess the lateromedial organization of r5 precursors, we used two different dyes to label both regions within a single embryo (n = 3). An example of a double-labeled hindbrain is shown in Fig. 4. Figure 4A shows a schematic diagram of the E2 embryo, with a DiI injection in the lateral part of r5 shown in red and a DiD injection into the medial part of r5 shown in green. In Fig. 4B, the E2 embryo is shown just after injection with DiI (bright spot) and DiD (dark spot) into the lateral and medial halves, respectively, of r5. Figure 4C shows a section through the brain stem of the same embryo after survival to E11, imaged using confocal microscopy, with DiI rendered in red and DiD rendered in green. The

FIG. 5. Lateral and medial regions of r6 contribute to lateral and medial regions of NM and NL. (A) Schematic illustration of medial r6 injection. (B) E2 embryo injected with DiI into the medial half of left r6. Scale bar, 200 μm. (C) Left side of a caudal brain-stem section from the embryo shown in B after survival to E9. Numerous labeled cells are present in NM and a few cells are labeled in NL. The label is largely confined to the medial portions of these nuclei. Arrows indicate the region of NM and the arrowhead indicates a labeled cell in the medial region of NL. Scale bar, 100 μm. (D) Schematic illustration of a lateral r6 injection. (E) An E2 embryo after injection into the lateral half of left r6. Scale bar, 200 μm. (F) The left side of the brain stem of the embryo in (E) at E9. NM (arrows) is heavily labeled. Arrowheads indicate two clusters of labeled NL cells. The label is heaviest in the lateral regions of both nuclei. Scale bar, 100 μm.

FIG. 6. Results from injections into quadrants of r6. (A) Schematic illustration of a lateral anterior r6 injection. (B) An E2 embryo after injection (arrow) into the lateral anterior quadrant of r6. (C) Left side of a coronal section through the brain stem of the embryo shown in (B) after survival to E12. NM cells (arrowheads) are labeled and are more numerous in the lateral region of the nucleus. NL cells are not labeled. Scale bar, 100 μm. (D) Schematic illustration of a DiI injection into the medial posterior quadrant of r6. (E) An E2 embryo that has been injected in the medial posterior quadrant of r6 (arrow). Scale bar, 200 μm; also applies to (B). (F) Section through the brain stem of the embryo shown in (E) after survival to E12. NM is outlined in dotted lines. A few medial NM cells are labeled with DiI (arrowheads). NL is not labeled. Scale bar, 100 μm.

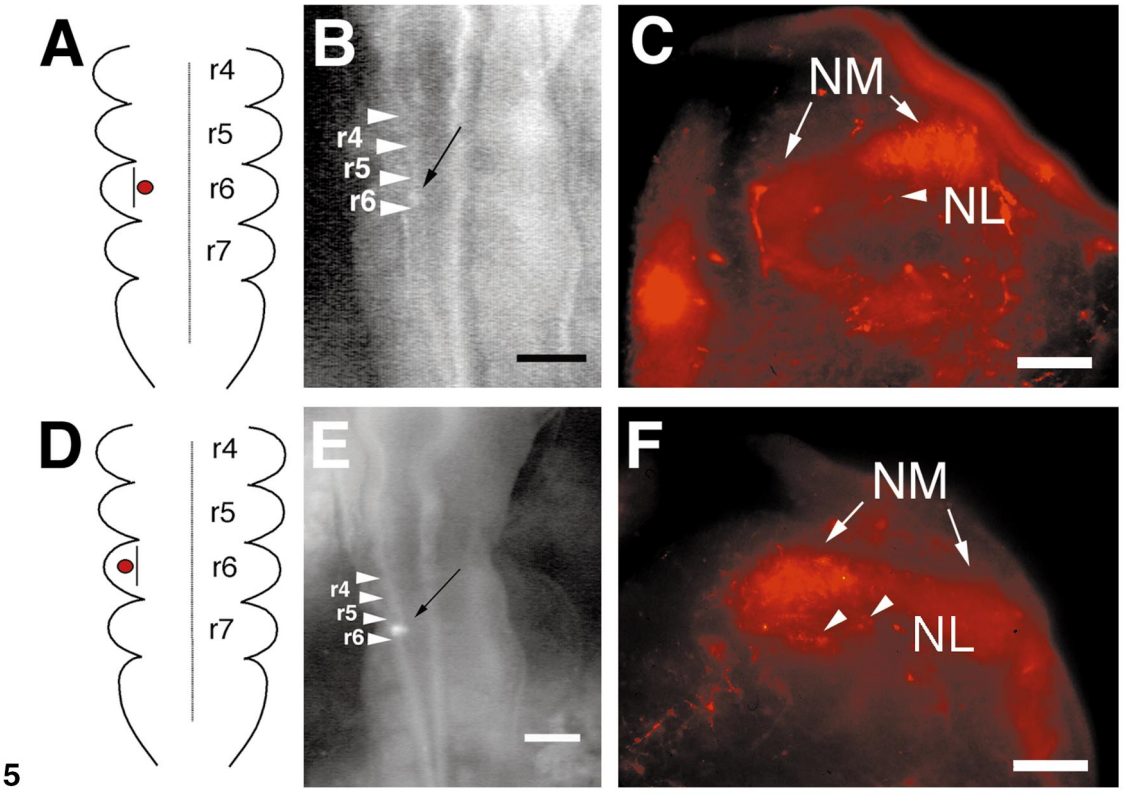

5

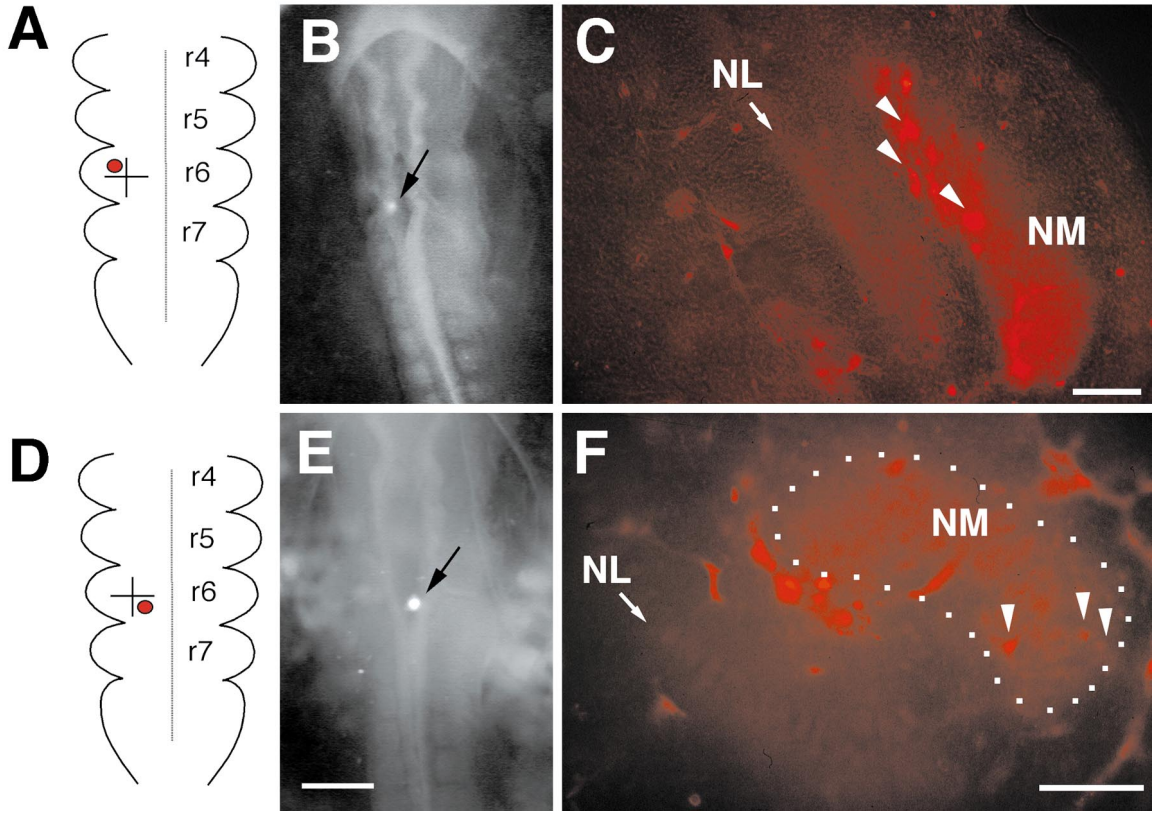

6

TABLE 2
Fates of Rhombomere 5 Cells

Injection site	Label in brain stem	
	NM	NL
Lateral		
Anterior	−	±
	−	−
	−	+
	−	+
	−	±
Middle[a]	−	+
	−	+
	−	±
	−	+
Posterior	−	+
	−	+
	−	+
	−	−
Medial		
Anterior	+	−
	+	±
	±	−
Middle[a]	+	−
	+	+
	+	−
Posterior	+	−
	+	−
	+	−
	+	−

Note. Scoring: −, no labeled cells; ±, few labeled cells; +, many labeled cells.

[a] Half-rhombomere injections are designated as "middle" with respect to the anteroposterior axis.

double-labeled areas appear yellow, and these are mostly accounted for by autofluorescence in blood vessels. Within NM and NL, labeling was largely nonoverlapping, confirming that NL arises from the lateral (DiI injected) area of the early hindbrain while NM arises from the medial (DiD injected) area. The separation of DiI and DiD labeling in these embryos persisted throughout the rostrocaudal extent of these nuclei in the brain stem. We obtained similar results suggesting that lateral r5 precursors give rise to NL and medial precursors to NM when the relative positions of the two dyes were switched, ruling out any artifact related to the dyes. These results confirm that the partitioning of precursors occurs within individual embryos.

The segregation of precursors for NM and NL in r5 prompted us to examine the organization of precursors for other nuclei in experiments carried out later in the study. Following injections into quadrants or halves of r5, the contributions to NA and SON were assessed in a subset of the embryos. Precursors for NA tended to be located in lateral regions of the rhombomere, while precursors for SON arose from both regions with a preference for medial precursors. Five of the embryos with lateral r5 injections ($n = 6$) had labeled cells in NA, while only three had labeled cells in SON. No embryos with medial r5 injections ($n = 8$) had labeled cells in NA. Seven of these had labeled cells in SON. Rhombomere 5 precursors thus contribute to all the auditory brain-stem nuclei. The fates of lateral r5 precursors are preferentially within NL and NA, while the fates of medial r5 precursors are preferentially within NM and SON.

The rostrocaudal labeling index is a measure of the mean rostrocaudal position of labeled descendants (see Materials and Methods) within the nuclei NM and NL. For all analyzed r5 injections, the index for NL, I_{NL}, was 1.20 ± 0.25 ($n = 9$ embryos with labeled cells in NL), and I_{NM} was 1.35 ± 0.35 ($n = 8$ embryos with labeled cells in NM). When anterior and posterior injections were analyzed separately, I_{NL} was 1.0 ± 0 for anterior r5 injections ($n = 3$) and 1.33 ± 0.24 for posterior r5 injections ($n = 4$). I_{NM} was 1.5 ± 0 for anterior r5 injections ($n = 2$) and 1.125 ± 0.25 for posterior r5 injections ($n = 4$). These measurements give an indication of the region of NM or NL labeled following precursor injections and suggest that r5 precursors give rise to the rostral regions of NM and NL.

Rhombomere 6

Injections that filled most of r6 in E2 embryos ($n = 4$) resulted in abundant labeling of NM cells at E9–E12. Table 1 summarizes the results from whole-rhombomere injections into r6. In some cases most of the cells in NM were labeled. Very few NL cells were labeled. NL cell labeling was occasionally seen but was always much less abundant than that seen following DiI injections into r5. Injections into r6 also resulted in labeling in VeM, VeD, nucleus of the IXth nerve, and in some cases a small number of cells in NA.

Focal injections were made into smaller regions within the rhombomere. Within r6, one embryo was injected in the medial half of the rhombomere (Figs. 5A, 5B, and 5C) and one was injected in the lateral half (Figs. 5D, 5E, and 5F). In addition, three embryos were injected in the lateral anterior quadrant, two were injected in the lateral posterior quadrant, one was injected in the medial anterior quadrant, and three were injected in the medial posterior quadrant. R6 injections resulted in NM label in 9 of these 11 focal injection cases. The half-rhombomere injections resulted in a few labeled cells in NL (Fig. 5), while none of the quadrant injections resulted in NL label. Figure 6 shows an example of a lateral anterior r6 injection (Figs. 6A and 6B) with resulting label (Fig. 6C) in the lateral portion of NM and no label in NL. In addition, an injection into the medial posterior quadrant of r6 (Figs. 6D and 6E) resulted in labeled cells in the medial region of NM but no labeled cells in NL. Lateral r6 injections resulted in abundant DiI labeling predominantly in lateral portions of NM (and a few cells in lateral portions of NL), particularly in the caudal regions of the nuclei. Medial r6 injections resulted in label that was

predominantly in the medial portions of NM and a few cells in the medial portion of NL. Within r6, it appears that there is a mediolateral organization to the precursors that is reflected in the positions of descendant cells in the mature nuclei.

Rostrocaudal labeling indices were computed for label following injection into r6. For all analyzed r6 cases, I_{NL} was 2.0 ± 0 (n = 3 embryos with labeled cells in NL) and I_{NM} was 2.4 ± 0.38 (n = 10 embryos with labeled cells in NM). For injections into anterior r6, I_{NM} was 2.33 ± 0.29 (n = 3). For injections into posterior r6, I_{NM} was 2.77 ± 0.40 (n = 3). Injections restricted to the anterior or posterior half of r6 did not result in labeled cells in NL; thus I_{NL} was not computed for these small injections.

Rhombomere 7

DiI injections into r7 were made in three embryos. In E2–E2.5 embryos, it was difficult to identify precisely the boundary between rhombomeres 7 and 8, although the boundary between rhombomeres 6 and 7 was distinct. The caudal boundary could be vaguely discerned as a broad indentation. To ensure labeling of r7, two r7 injections were made reasonably close to the r6/r7 boundary. None of the r7 injections resulted in any labeled cells in NL. Labeling in NM was abundant only in the caudalmost region of NM, a level at which NL was no longer present. Labeled cells in these embryos continued through the long caudal tail of NM. Labeled cells were also observed in VeM, as well as diffusely in ventral regions of the brain stem in some sections. In the most caudal sections, labeling in nuclei other than NM was not observed. An example is shown in Fig. 7. In r7 injections, two embryos were analyzed for rostrocaudal topography; I_{NM} was 3.0 ± 0.

Topography of Precursors for NM and NL

An analysis was undertaken to investigate whether the relative rostrocaudal positions of NM and NL precursors in the hindbrain are preserved in the brain stem when the nuclei have differentiated. For this analysis, 28 of the 45 embryos used in the study were analyzed. Of these 28 embryos, 12 had labeled cells in NL and 20 had labeled cells in NM. Injections were given values according to their rostrocaudal positions within the hindbrain (see Materials and Methods). The rostrocaudal distribution of labeled cells in NM and NL (I_{NM} and I_{NL}) was then quantified at E9–12 (see above for values for each rhombomere injection). Using a Spearman's rank correlation to evaluate the correlation between injection position and I_{NM} and I_{NL} in the differentiated brain-stem nuclei, we found highly significant correlations relating the rostrocaudal positions of precursors to the rostrocaudal positions of descendants within both NM and NL. For NM, $\rho = 0.812$; $P < 0.005$. For NL, $\rho = 0.846$; $P < 0.005$. These correlations are strong when data from all contributing rhombomeres (5, 6, and 7) are included. However, topography in the contributions within rhombomeres 5 and 6 was not significant except in the r6 contributions to NM, in which $\rho = 0.667$; $P < 0.05$. These distributions are represented graphically in Fig. 8.

DISCUSSION

This study provides a detailed analysis of the fate map of the auditory nuclei in the chick hindbrain with particular emphasis on the formation of the auditory brain-stem nuclei NM and NL. We have used lipophilic dye injections to label groups of cells within rhombomeres. Our approach allowed us to label small regions within rhombomeres to assess the topographic arrangement of precursors in small regions of the hindbrain and to address the issue of lineage relationships between these nuclei. A summary of the data obtained in this study is represented schematically in Fig. 9. Colored areas of the schematized E2 embryo on the left have descendants in matching colored areas within the schematic brain-stem sections on the right. We found that NM and NL arise from several rhombomeres and that r5 and r6 contribute to both NM and NL. Within r5, the precursors for NM cells are spatially distinct from the precursors for NL cells, with medial regions contributing to NM and lateral regions contributing to NL. Similarly, NA cells arise from r4 and from lateral precursors in r5. SON cells also arise from r5. Medial injections resulted in SON label in 87% of the cases studied, while lateral injections labeled SON in 60% of the cases.

Fate-mapping studies have been carried out previously using lipophilic dyes to label small groups of cells in chicks (Sechrist *et al.*, 1993; Birgbauer and Fraser, 1994; Birgbauer *et al.*, 1995), as well as in mice (Shuler *et al.*, 1992; Sulik *et al.*, 1994; Wilson and Beddington, 1996), sea urchins (Logan and McClay, 1997; Ransick and Davidson, 1998), fruitflies (Bossing and Technau, 1994; Bossing *et al.*, 1996), and other organisms (Eagleson *et al.*, 1995; Cruz *et al.*, 1996). Although it is in principle possible for dye to spread to other areas via contacts between membranes, such spread does not seem likely in our tissue for several reasons. First, following the injection, we observed very little spread of the dye, even after 24 h. Second, no labeling was observed in remote areas with known connections to labeled areas. Third, our results were overall quite similar to studies of quail/chick chimeras, in which rhombomere descendants are arranged in anteromedial to posterolateral columns (Marin and Puelles, 1995). A concern about DiI labeling is that because the dye is membrane soluble, labeling might diminish significantly after several cell divisions. For this reason, dye injections were made less than 24 h before the final mitotic divisions of cells contributing to NM (Rubel *et al.*, 1976), limiting the number of cell divisions that would result in dilution of the dye. Labeling in NL might appear to have lower levels than labeling in NM because NL is a sheet of cells that is one cell thick in most places. In addition, NM cells are larger than NL cells and may appear brighter. Because NL cells are born later than NM cells (Rubel *et al.*, 1976), it is possible that NL cells are less bright because the

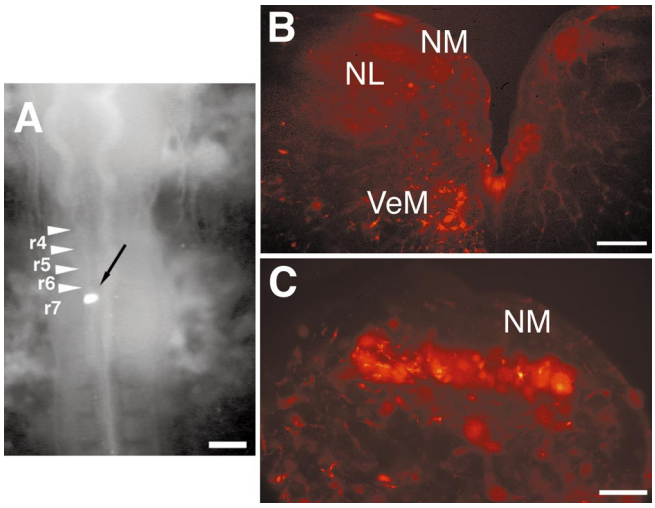

FIG. 7. (A) An E2 embryo injected with DiI into r7 on the left side. Scale bar, 200 μm. (B) Middle section through the brain stem of the same embryo after survival to E10. No DiI-labeled cells are seen in NM or NL at this level of the brain stem. Scale bar, 200 μm. (C) Left side of a caudal section through this brain stem. NM cells are heavily labeled with DiI. Scale bar, 100 μm.

dye is diluted by cell division. However, we do not feel that this is a major concern for several reasons. First, we find similar results, and similar NL labeling, when injections are made at E2 or E2.5. Second, the presence of NL labeling resulting from lateral r5 injections is a positive control showing that NL cells can be adequately labeled by applying dye to precursors. The labeling in Figs. 3C and 3F shows that NL cells can be quite intensely labeled following injection at E2. Finally, the results we obtained for r5 quadrant injections were quite consistent and were supported by experiments in which medial and lateral regions were injected in a single embryo. While it is in principle possible for lateral r5 (NL) precursors to migrate to medial r5 between injection time and birth date (i.e., final cell division), our data show that at the time of injection (approximately 24 h before the last cell division) injections in the medial part of r5 do not label cells that will ultimately become NL cells.

Previous studies addressing the fate map of the chick hindbrain have focused on quail/chick chimeras in which grafts of quail rhombomeres are placed in a chick (or vice versa), and the progeny of grafted cells are located in the later embryo using immunohistochemical localization of the donor cells (Tan and Le Douarin, 1991; Marin and Puelles, 1995). While we have used a different method in order to examine the fate map, our results are largely in agreement with those of previous studies. We found that both NM and NL arise from the alar region of the neural plate, in agreement with Tan and LeDouarin (1991). The rhombomeric origins of auditory and vestibular nuclei we describe are similar to those reported by Marin and Puelles (1995). The major difference between the studies is that we found a substantial contribution to both NL and NM from r5, while the previous study found no r5 grafted cells in NM (Marin and Puelles, 1995). It is possible that this disparity results from differences in the methods used. One possibility is that in the earlier study only the lateral region of the grafted rhombomere survived the grafting procedure and subsequently the cells in this lateral region followed their normal fates in the host embryo, resulting in progeny within NL but not NM. Another possibility is that quail cells may follow different fates or may behave differently when grafted. The chick/quail chimera technique likely requires some time for healing of the tissue subsequent to grafting. Given that several regions contribute to NM, it is possible that grafted medial r5 cells fail to commence migration at the appropriate time because of the time required for healing. Nonetheless, the overall agreement between the two studies supports the appropriateness of both methods for mapping fates of whole rhombomeres. Our results extend the existing knowledge of the fate map of the hindbrain and shed some new light on how individual nuclei form from the group of precursors found within individual rhombomeres.

The distinct locations of the precursors for NM and NL, particularly within r5, suggest that these precursors follow distinct migratory pathways during the formation of the mature nuclei, even when the cells making up the nuclei are grouped as a common anlage. Preliminary experiments suggest that small injections within r5 result in label in a confined region within the auditory anlage (unpublished observations). Future experiments will examine the migratory pathways in detail at various time points following injection.

Rhombomeres confer a general rostrocaudal plan to the developing brain-stem nuclei. Rhombomeric origin is re-

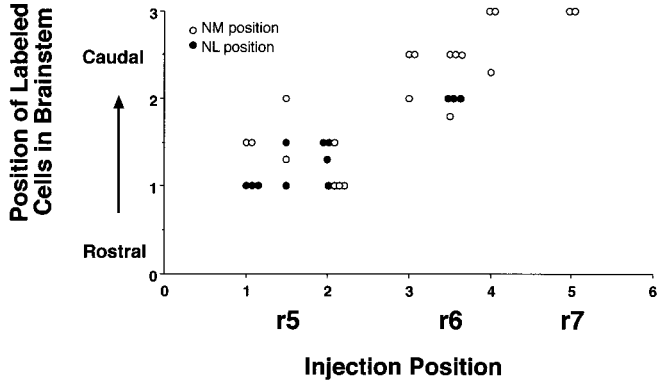

FIG. 8. Scatter plot comparing the position of the injection site (x axis) with the position of labeled cells in NM or NL. Overlapping points have been shifted slightly so that all points are visible. Injection position was assigned a value (see text), and position of label was scored for rostral sections, in which NL was largely lateral to NM; middle sections, in which NL was ventral to NM; and caudal sections, which contained NM but not NL. Each point represents data for a single nucleus from a single embryo.

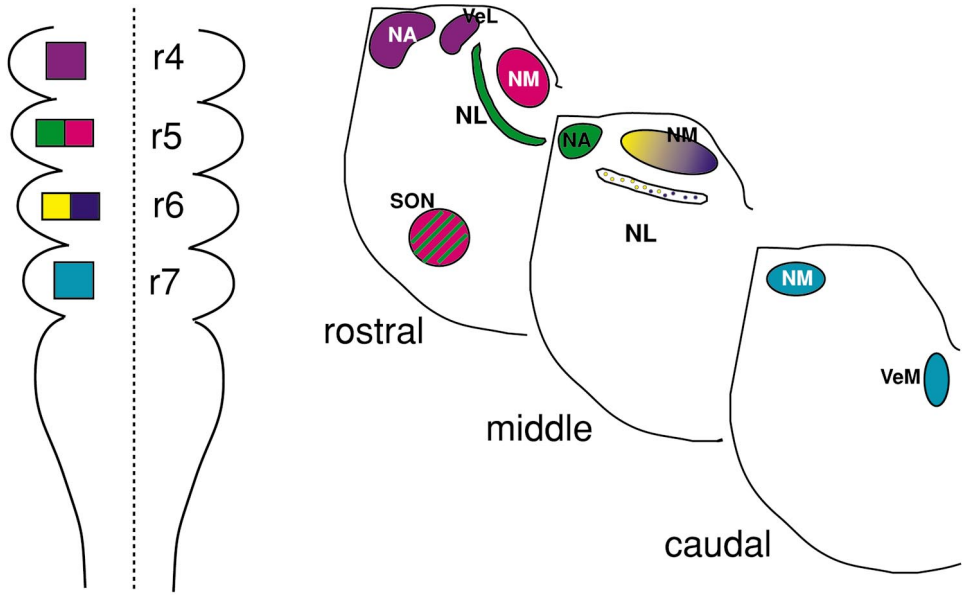

FIG. 9. Summary of fate map data obtained using small DiI injections into regions of rhombomeres in E2–E2.5 chick embryos. Label was identified in E9–E12 embryos in coronal sections. Cells in r4 contribute to NA, but not to NM or NL. In rostral regions of the brain stem, NM is largely medial to NL. Medial r5 precursors give rise to NM but contribute very little to NL, while lateral r5 precursors contribute to NL but not to NM. R5 also contributes to SON and lateral precursors within r5 contribute to NA. In the middle sections, NM is largely dorsal to NL, and both nuclei have their long axes mediolaterally. Here, medial and lateral precursors of r6 give rise to medial and lateral regions within the nuclei, with very little labeling in NL. R7 contributes to NM in caudal sections that do not contain NL.

lated to overall position of cells within the nuclei NM and NL. In particular, NM cells vary in morphology between the rostral and the caudal regions (Rubel and Parks, 1975; Jhaveri and Morest, 1982a). Some of these cells may correspond to NM contributions from r7, which contributes only to the long portion of NM that is completely caudal to NL. An intriguing possibility is that the frequency tuning of cells in NM and NL is related to the positions of precursors within the hindbrain. While our study did not address this issue directly, the strong correlation between the positions of all injection sites and the rostrocaudal position of labeled neurons is supportive of this idea.

Despite the rostrocaudal topography relating early precursors to later positions within mature nuclei, our results indicate that rhombomeric boundaries do not constitute boundaries between precursors contributing to individual brain-stem nuclei. The auditory brain-stem nuclei arise from multiple rhombomeres in the chick hindbrain. This finding is consistent with previous results (Tan and Le Douarin, 1991; Marin and Puelles, 1995). Thus it appears that some nuclei are the progeny of cells confined to a single rhombomere (such as SON), while other nuclei have contributions from two or more rhombomeres. The variability in the number of contributing rhombomeres has also been shown in vestibular neuron projection groups (Diaz *et al.*, 1998), which are defined by projection patterns rather than by boundaries of nuclei. The formation of NM and NL occurs over a fairly long period, during which postmitotic neurons migrate to appropriate locations and become distinct from each other. Cells that contribute to NM and NL are born during a stage when rhombomeres and rhombomere boundaries are present (Rubel *et al.*, 1976). While rhombomere boundaries limit migration, there remains a small proportion of cells (about 15%) that cross rhombomere boundaries (Birgbauer and Fraser, 1994). In addition, migration is not complete until about E10–11, nearly a week after rhombomere boundaries disappear, although some rhombomeric specification, particularly in ventricular areas, may persist until E9 (Wingate and Lumsden, 1996). The lack of sharp boundaries between areas of different rhombomeric origin is consistent with the extended period of migration. Thus, the rostrocaudal positions of precursors, but not rhombomere boundaries per se, influence the positions of descendants within the auditory brain-stem nuclei.

In addition to rostrocaudal topography, we found significant differences in the progeny of lateral versus medial regions within rhombomeres. Rhombomere 5 makes the most substantial contribution to NL. In this rhombomere, the lateral region of the alar plate contributes to NL, while the medial region makes a substantial contribution to NM. Rostral sections of the auditory brain stem receive the largest r5 contribution. In this region, NL is lateral to NM, and thus the arrangement of precursors is topographically

related to the positions of the mature nuclei. Rhombomere 5 thus contains distinct pools of precursors for NM and NL. This finding rules out the possibility that NM and NL arise from common precursors and suggests instead that the precursors are determined in relation to their position prior to E2. Thus, it is unlikely that cells in NM and NL arise from a common set of precursors, despite their emergence from a common anlage and the highly precise map of projections from NM to NL. In addition, lateromedial positions of precursors within r5 are related to the positions of NA, which is lateral in the mature brain stem, and SON, which is somewhat more medial than NA. Rhombomere 6 contributes substantially to more caudal regions of NM and only slightly to NL. In r6, the lateromedial position of the injection is directly related to the lateromedial position of labeled cells in the mature NM and NL. This order also preserves the topographic arrangement for NM and NL in their caudal regions where NM is dorsal to NL. While a lineage relationship remains possible in the regions of NM and NL derived from r6, the contribution from r6 to NL is substantially smaller than that of r5, and any lineage relationship would constitute a minority of cells in NL.

The final mitotic divisions of cells that contribute to NM and NL occur at nonoverlapping periods of development, with all NM cells born prior to all NL cells (Rubel *et al.*, 1976). While it has been reported that neurons differentiate in even-numbered rhombomeres earlier than in odd-numbered rhombomeres (Lumsden and Keynes, 1989), the fate map of NM and NL precursors suggests that there are regional differences within rhombomeres that dictate the birth dates of neurons. Marin and Puelles (1995) report that the caudalmost segment of NM, which is derived from r7, is born earlier than the rest of NM, suggesting that rhombomeric origin may influence birth dates within a nucleus as well. In the mature brain stem NL cells are largely ventral to NM. Because of their later birth dates within the ventricular zone, it was proposed that NL cells must migrate through the nascent NM in order to arrive at their final position (Rubel *et al.*, 1976). However, our results pose the possibility that the medially located NM precursors in r5 have a longer migratory course to the lateral anlage, which may compensate for their earlier birth dates. Thus, NL cells may reach their destination before NM cells have coalesced within the anlage. Detailed studies of the migratory routes of NM and NL precursors will shed light on this issue.

ACKNOWLEDGMENTS

Preliminary studies while E.WR. was on sabbatical at Caltech were supported in part by a Wiersma Fellowship. We are grateful to Drs. M. Bronner-Fraser, P. Kulesa, and M. Konishi for valuable suggestions during this study. We are also grateful to G. MacDonald for technical assistance and to D. Molea, Dr. L. Westrum, and Dr. O. Bermingham-McDonogh for helpful suggestions with this study. In addition, we thank Drs. S. Cochran and L. Cunningham for helpful comments on the manuscript. This research was supported by NIH 00395.

REFERENCES

Birgbauer, E., and Fraser, S. E. (1994). Violation of cell lineage restriction compartments in the chick hindbrain. *Development* **120,** 1347–1356.

Birgbauer, E., Sechrist, J., Bronner-Fraser, M., and Fraser, S. (1995). Rhombomeric origin and rostrocaudal reassortment of neural crest cells revealed by intravital microscopy. *Development* **121,** 935–945.

Book, K. J., and Morest, D. K. (1990). Migration of neuroblasts by perikaryal translocation: Role of cellular elongation and axonal outgrowth in the acoustic nuclei of the chick embryo medulla. *J. Comp. Neurol.* **297,** 55–76.

Bossing, T., and Technau, G. M. (1994). The fate of the CNS midline progenitors in Drosophila as revealed by a new method for single cell labelling. *Development* **120,** 1895–1906.

Bossing, T., Technau, G. M., and Doe, C. Q. (1996). huckebein is required for glial development and axon pathfinding in the neuroblast 1-1 and neuroblast 2-2 lineages in the Drosophila central nervous system. *Mech. Dev.* **55,** 53–64.

Carr, C. E., and Boudreau, R. E. (1993). Organization of the nucleus magnocellularis and the nucleus laminaris in the barn owl: Encoding and measuring interaural time differences. *J. Comp. Neurol.* **334,** 337–355.

Carr, C. E., Fujita, I., and Konishi, M. (1989). Distribution of GABAergic neurons and terminals in the auditory system of the barn owl. *J. Comp. Neurol.* **286,** 190–207.

Cruz, Y. P., Yousef, A., and Selwood, L. (1996). Fate-map analysis of the epiblast of the dasyurid marsupial Sminthopsis macroura (Gould). *Reprod. Fertil. Dev.* **8,** 779–788.

Diaz, C., Puelles, L., Marin, F., and Glover, J. C. (1998). The relationship between rhombomeres and vestibular neuron populations as assessed in quail–chicken chimeras. *Dev. Biol.* **202,** 14–28.

Eagleson, G., Ferreiro, B., and Harris, W. A. (1995). Fate of the anterior neural ridge and the morphogenesis of the Xenopus forebrain. *J. Neurobiol.* **28,** 146–158.

Fraser, S., Keynes, R., and Lumsden, A. (1990). Segmentation in the chick embryo hindbrain is defined by cell lineage restrictions. *Nature* **344,** 431–435.

Fraser, S. E. (1996). Iontophoretic dye labeling of embryonic cells. *In* "Methods in Cell Biology" (M. Bronner-Fraser, Ed.), Vol. 51, pp. 147–160. Academic Press, San Diego.

Hackett, J. T., Jackson, H., and Rubel, E. W. (1982). Synaptic excitation of the second and third order auditory neurons in the avian brain stem. *Neuroscience* **7,** 1455–1469.

Hamburger, V., and Hamilton, H. (1951). A series of normal stages in the development of the chick embryo. *J. Morphol.* **88,** 49–92.

Harkmark, W. (1954). Cell migrations from the rhombic lip to the inferior olive, the nucleus raphe and pons. A morphological and experimental investigation on chick embryos. *J. Comp. Neurol.* **100,** 115–209.

Hunt, P., and Krumlauf, R. (1992). Hox codes and positional specification in vertebrate embryonic axes. *Annu. Rev. Cell Biol.* **8,** 227–256.

Jhaveri, S., and Morest, D. K. (1982a). Neuronal architecture in nucleus magnocellularis of the chicken auditory system with observations on nucleus laminaris: A light and electron microscope study. *Neuroscience* **7,** 809–836.

Jhaveri, S., and Morest, D. K. (1982b). Sequential alterations of neuronal architecture in nucleus magnocellularis of the developing chicken: A Golgi study. *Neuroscience* **7,** 837–853.

Lachica, E. A., Rubsamen, R., and Rubel, E. W. (1994). GABAergic terminals in nucleus magnocellularis and laminaris originate from the superior olivary nucleus. *J. Comp. Neurol.* **348,** 403–418.

Logan, C. Y., and McClay, D. R. (1997). The allocation of early blastomeres to the ectoderm and endoderm is variable in the sea urchin embryo. *Development* **124,** 2213–2223.

Lumsden, A., and Keynes, R. (1989). Segmental patterns of neuronal development in the chick hindbrain. *Nature* **337,** 424–428.

Marin, F., and Puelles, L. (1995). Morphological fate of rhombomeres in quail/chick chimeras: A segmental analysis of hindbrain nuclei. *Eur. J. Neurosci.* **7,** 1714–1738.

McKay, I. J., Muchamore, I., Krumlauf, R., Maden, M., Lumsden, A., and Lewis, J. (1994). The kreisler mouse: A hindbrain segmentation mutant that lacks two rhombomeres. *Development* **120,** 2199–2211.

Moiseff, A., and Konishi, M. (1983). Binaural characteristics of units in the owl's brainstem auditory pathway: Precursors of restricted spatial receptive fields. *J. Neurosci.* **3,** 2553–2562.

Monsivais, P., Yang, L., and Rubel, E. W. (2000). GABAergic inhibition in nucleus magnocellularis: Implications for phase locking in the avian auditory brainstem. *J. Neurosci.* **20,** 2954–2963.

Nonchev, S., Maconochie, M., Vesque, C., Aparicio, S., Ariza-McNaughton, L., Manzanares, M., Maruthainar, K., Kuroiwa, A., Brenner, S., Charnay, P., and Krumlauf, R. (1996). The conserved role of Krox-20 in directing Hox gene expression during vertebrate hindbrain segmentation. *Proc. Natl. Acad. Sci. USA* **93,** 9339–9345.

Overholt, E. M., Rubel, E. W., and Hyson, R. L. (1992). A circuit for coding interaural time differences in the chick brainstem. *J. Neurosci.* **12,** 1698–1708.

Parks, T. N. (1981). Morphology of axosomatic endings in an avian cochlear nucleus: Nucleus magnocellularis of the chicken. *J. Comp. Neurol.* **203,** 425–440.

Parks, T. N., and Rubel, E. W. (1975). Organization and development of brain stem auditory nuclei of the chicken: Organization of projections from n. magnocellularis to n. laminaris. *J. Comp. Neurol.* **164,** 435–448.

Parks, T. N., and Rubel, E. W. (1978). Organization and development of the brain stem auditory nuclei of the chicken: Primary afferent projections. *J. Comp. Neurol.* **180,** 439–448.

Ransick, A., and Davidson, E. H. (1998). Late specification of Veg1 lineages to endodermal fate in the sea urchin embryo. *Dev. Biol.* **195,** 38–48.

Rubel, E. W. (1978). Ontogeny of structure and function in the vertebrate auditory system. *In* "Handbook of Sensory Physiology," Vol. IX, "Development of Sensory Systems" (M. Jacobson, Ed.), pp. 135–237. Springer-Verlag, Berlin.

Rubel, E. W., and Parks, T. N. (1975). Organization and development of brain stem auditory nuclei of the chicken: Tonotopic organization of n. magnocellularis and n. laminaris. *J. Comp. Neurol.* **164,** 411–433.

Rubel, E. W., and Parks, T. N. (1988). Organization and development of the avian brain-stem auditory system. *In* "Auditory Function: The Neurobiological Basis of Hearing" (G. M. Edelman, W. E. Gall, and W. M. Cowan, Eds.), pp. 3–92. Wiley, New York.

Rubel, E. W., Smith, D. J., and Miller, L. C. (1976). Organization and development of brain stem auditory nuclei of the chicken: Ontogeny of n. magnocellularis and n. laminaris. *J. Comp. Neurol.* **166,** 469–490.

Schwarz, D. W. (1992). Sound delay lines in the nucleus laminaris of the chicken. *J. Otolaryngol.* **21,** 202–208.

Sechrist, J., Serbedzija, G. N., Scherson, T., Fraser, S. E., and Bronner-Fraser, M. (1993). Segmental migration of the hindbrain neural crest does not arise from its segmental generation. *Development* **118,** 691–703.

Shuler, C. F., Halpern, D. E., Guo, Y., and Sank, A. C. (1992). Medial edge epithelium fate traced by cell lineage analysis during epithelial–mesenchymal transformation *in vivo*. *Dev. Biol.* **154,** 318–330.

Smith, D. J., and Rubel, E. W. (1979). Organization and development of brain stem auditory nuclei of the chicken: Dendritic gradients in nucleus laminaris. *J. Comp. Neurol.* **186,** 213–239.

Sulik, K., Dehart, D. B., Iangaki, T., Carson, J. L., Vrablic, T., Gesteland, K., and Schoenwolf, G. C. (1994). Morphogenesis of the murine node and notochordal plate. *Dev. Dyn.* **201,** 260–278.

Sullivan, W. E., and Konishi, M. (1986). Neural map of interaural phase difference in the owl's brainstem. *Proc. Natl. Acad. Sci. USA* **83,** 8400–8404.

Takahashi, T., Moiseff, A., and Konishi, M. (1984). Time and intensity cues are processed independently in the auditory system of the owl. *J. Neurosci.* **4,** 1781–1786.

Takahashi, T. T., and Konishi, M. (1988). Projections of nucleus angularis and nucleus laminaris to the lateral lemniscal nuclear complex of the barn owl. *J. Comp. Neurol.* **274,** 212–238.

Tan, K., and Le Douarin, N. M. (1991). Development of the nuclei and cell migration in the medulla oblongata. Application of the quail–chick chimera system. *Anat. Embryol.* **183,** 321–343.

Vaage, S. (1969). The segmentation of the primitive neural tube in chick embryos (Gallus domesticus). *Adv. Anat. Embryol. Cell Biol.* **41,** 1–88.

Westerberg, B. D., and Schwarz, D. W. (1995). Connections of the superior olive in the chicken. *J. Otolaryngol.* **24,** 20–30.

Wilkinson, D. G., Bhatt, S., Cook, M., Boncinelli, E., and Krumlauf, R. (1989). Segmental expression of Hox-2 homeobox-containing genes in the developing mouse hindbrain. *Nature* **341,** 405–409.

Wilson, V., and Beddington, R. S. (1996). Cell fate and morphogenetic movement in the late mouse primitive streak. *Mech. Dev.* **55,** 79–89.

Wingate, R. J., and Lumsden, A. (1996). Persistence of rhombomeric organisation in the postsegmental hindbrain. *Development* **122,** 2143–2152.

Yang, L., Monsivais, P., and Rubel, E. W. (1999). The superior olivary nucleus and its influence on nucleus laminaris: A source of inhibitory feedback for coincidence detection in the avian auditory brainstem. *J. Neurosci.* **19,** 2313–2325.

Young, S. R., and Rubel, E. W. (1983). Frequency-specific projections of individual neurons in chick brainstem auditory nuclei. *J. Neurosci.* **3,** 1373–1378.

Received for publication January 3, 2000
Revised May 11, 2000
Accepted May 11, 2000